

Accepted for publication in *Ap.J.* August 2, 2001

First Simultaneous Optical and EUV Observations of the Quasi-Coherent Oscillations of SS Cygni

Christopher W. Mauche

Lawrence Livermore National Laboratory, L-43, 7000 East Avenue, Livermore, CA 94550;
mauche@cygnus.llnl.gov

and

Edward L. Robinson

Department of Astronomy, University of Texas, Austin, TX 78712;
elr@astro.as.utexas.edu

ABSTRACT

Using EUV photometry obtained with the *Extreme Ultraviolet Explorer (EUVE)* satellite and *UBVR* optical photometry obtained with the 2.7-m telescope at McDonald Observatory, we have detected quasi-coherent oscillations (so-called “dwarf nova oscillations”) in the EUV and optical flux of the dwarf nova SS Cygni during its 1996 October outburst. There are two new results from these observations. First, we have for the first time observed “frequency doubling:” during the rising branch of the outburst, the period of the EUV oscillation was observed to *jump* from 6.59 s to 2.91 s. Second, we have for the first time observed quasi-coherent oscillations *simultaneously* in the optical and EUV. We find that the period and phase of the oscillations are the same in the two wavebands, finally confirming the long-held assumption that the periods of the optical and EUV/soft X-ray oscillations of dwarf novae are equal. The *UBV* oscillations can be simply the Rayleigh-Jeans tail of the EUV oscillations if the boundary layer temperature $kT_{\text{bb}} \lesssim 15$ eV and hence the luminosity $L_{\text{bb}} \gtrsim 1.2 \times 10^{34} (d/75 \text{ pc})^2 \text{ erg s}^{-1}$ (comparable to that of the accretion disk). Otherwise, the lack of a phase delay between the EUV and optical oscillations requires that the optical reprocessing site lies within the inner third of the accretion disk. This is strikingly different from other cataclysmic variables, where much or all of the disk contributes to the optical oscillations.

Subject headings: novae, cataclysmic variables — stars: individual (SS Cygni) — stars: oscillations — ultraviolet: stars

1. Introduction

Rapid periodic oscillations are observed in the optical flux of high accretion rate (“high- \dot{M} ”) cataclysmic variables (nova-like variables and dwarf novae in outburst) (Patterson 1981; Warner 1995a,b). These oscillations have high coherence ($Q \approx 10^4$ – 10^6), short periods ($P \approx 7$ – 40 s), low amplitudes ($A \lesssim 0.5\%$), and are sinusoidal to within the limits of measurement. They are referred to as “dwarf nova oscillations” (DNOs) to distinguish them from the apparently distinct longer period, low coherence ($Q \approx 1$ – 10) quasi-periodic oscillations (QPOs) of high- \dot{M} cataclysmic variables, and the longer period, high coherence ($Q \approx 10^{10}$ – 10^{12}) oscillations of DQ Her stars. DNOs appear on the rising branch of the dwarf nova outburst, typically persist through maximum, and disappear on the declining branch of the outburst. The period of the oscillation decreases on the rising branch and increases on the declining branch, but because the period reaches minimum about one day after maximum optical flux, dwarf novae describe a loop in a plot of oscillation period versus optical flux.

The dwarf nova SS Cygni routinely exhibits DNOs during outburst. Optical oscillations have been detected at various times with periods ranging from 7.3 s to 10.9 s (Patterson, Robinson, & Kiplinger 1978; Horne & Gomer 1980; Hildebrand, Spillar, & Stiening 1981; Patterson 1981). In the soft X-ray and EUV wavebands, quasi-coherent oscillations have been detected in *HEAO 1* LED 1 data at periods of 9 s and 11 s (Córdova et al. 1980, 1984), *EXOSAT* LE data at periods between 7.4 s and 10.4 s (Jones & Watson 1992), *EUVE* DS data at periods between 2.9 s and 9.3 s (Mauche 1996, 1998), and *ROSAT* HRI data at periods between 2.8 s and 2.9 s (van Teeseling 1997). Mauche (1996) showed that the period of the EUV oscillations of SS Cyg is a single-valued function of the EUV flux (hence, by inference, the mass-accretion rate onto the white dwarf), and explained the loops observed in plots of oscillation period versus optical flux as the result of the well-known delay between the rise of the optical and EUV flux at the beginning of dwarf nova outbursts. While the quasi-coherent oscillations of SS Cyg are usually sinusoidal to high degree, Mauche (1997) pointed out the pronounced distortion of the EUV waveform at the peak of the 1994 June/July outburst. We present here new observations in the optical and EUV obtained during the 1996 October outburst of SS Cyg.

2. Observations

2.1. EUVE

As discussed by Wheatley, Mauche, & Mattei (2000), AAVSO optical, *EUVE*, and *RXTE* observations of SS Cyg were obtained during a multiwavelength campaign in 1996 October designed to study the wavelength dependence of the outbursts of dwarf novae. The *EUVE* (Bowyer & Malina 1991; Bowyer et al. 1994) observations began on $JD - 2450000 = 366.402$ and ended on $JD - 2450000 = 379.446$. Data are acquired only during satellite night, which comes around

every 95 min and lasted for 23 min (at the beginning of the observation) to 32 min (at the end of the observation). Valid data are collected during intervals when various satellite housekeeping monitors [including detector background and primbsch/deadtime corrections] are within certain bounds. After discarding numerous short ($\Delta t \leq 10$ min) data intervals comprising less than 10% of the total exposure, we were left with a net exposure of 208 ks. EUV photometry is provided both by the deep survey (DS) photometer and short wavelength (SW) spectrometer, but the count rate is too low and the effective background is too high to detect oscillations in the SW data. Unfortunately, the DS photometer was switched off between October 11.37 UT and October 14.70 UT because the count rate was rising so rapidly on October 11 that the *EUVE* Science Planner feared that the DS instrument would be damaged while the satellite was left unattended over the October 12–13 weekend. We constructed an EUV light curve of the outburst from the background-subtracted count rates registered by the two instruments, using a 72–130 Å wavelength cut for the SW spectroscopic data, and applying an empirically-derived scale factor of 14.93 to the SW count rates to match the DS count rates. The resulting EUV light curve is shown by the filled symbols in the upper panel of Figure 1, superposed on the AAVSO optical light curve shown by the small dots (individual measurements) and histogram (half-day average). As shown by Mauche, Mattei, & Bateson (2001), the EUV light curve *lags* the optical light curve by $\approx 1\frac{1}{2}$ days during the rising branch of the outburst, then *leads* the optical light curve during the declining branch of the outburst. The secondary maximum of the EUV light curve at the very end of the optical outburst appears to be real, and coincides with the recovery of the hard X-rays flux measured by *RXTE* (Wheatley, Mauche, & Mattei 2000).

To determine the period of the oscillations of the EUV flux of SS Cyg, for each valid data interval we calculated the power spectra of the background-subtracted count rate light curves using 1.024 s bins (the bin width of the primbsch/deadtime correction table). Individual spectra typically consist of a spike superposed on a weak background due to Poisson noise, so in each case we took as the period of the oscillation the location of the peak of the power spectrum in the interval $\nu = 0.1$ –0.4 Hz ($P = 2.5$ –10 s). The resulting variation of the period of the EUV oscillation is shown in the lower panel of Figure 1. The oscillation was first convincingly detected on the rising branch of the outburst at a period of 7.81 s, fell to 6.59 s over an interval of 4.92 hr ($Q = 1.5 \times 10^4$), *jumped* to 2.91 s, and then fell to 2.85 s over an interval of 4.92 hr ($Q = 3.0 \times 10^5$) before observations with the DS were terminated. When DS observations resumed 3.4 days later during the declining branch of the outburst, the period of the EUV oscillation was observed to rise from 6.73 s to 8.23 s over an interval of 2.10 days ($Q = 1.2 \times 10^5$).

It is clear from the lower panel of Figure 1 that the period of the EUV oscillation of SS Cyg anticorrelates with the DS count rate, being long when the count rate is low and short when the count rate is high. To quantify this trend, we plot in Figure 2 the log of the period of the oscillation as a function of the log of the DS count rate. As in the previous figure, the data fall into two groups: one during the early rise (distinguished with crosses) and decline of the outburst, the other during the interval after the frequency of the oscillation had doubled. The trend during the early rise and

decline of the outburst is clearly the same; fitting a function of the form $P = P_0 I^{-\alpha}$, where I is the DS count rate, an unweighted fit to the data gives $P_0 = 7.26$ s and $\alpha = 0.097$. A similar fit to the data acquired after the oscillation frequency had doubled gives $P_0 = 2.99$ s and $\alpha = 0.021$. The first trend is consistent with that observed during outbursts of SS Cyg in 1993 August and 1994 June/July (Mauche 1996), but the trend after the frequency had doubled is clearly distinct: not only did the oscillation frequency double, its dependence on the DS count rate became “stiffer” by a factor of ≈ 5 in the exponent. SS Cyg seems to have been doing what it could to avoid oscillating faster than about 2.8 s. If this is the Keplerian period of material at the inner edge of the accretion disk, then $P_{\text{Kep}} \geq 2\pi(R_{\text{wd}}^3/GM_{\text{wd}})^{1/2} \approx 2.8$ s, requiring $M_{\text{wd}} \geq 1.27 M_{\odot}$ (assuming the Nauenberg 1972 white dwarf mass-radius relationship). If instead, $P_{\text{Kep}} \approx 5.6$ s (i.e., the observed 2.8 s period is the first harmonic of a 5.6 s Keplerian period), then $M_{\text{wd}} \gtrsim 1.08 M_{\odot}$. The data of Hessman et al. (1984), Friend et al. (1990), and Martínez-Pais et al. (1994) are consistent with a binary inclination $i \approx 40^\circ$ and white dwarf mass $M_{\text{wd}} = 0.9\text{--}1.1 M_{\odot}$, hence favor the second option, but it requires only a $\approx 10\%$ reduction in the inclination angle to accommodate the first option.

2.2. Optical

In an effort to obtain the first simultaneous optical and EUV/soft X-ray measurements of dwarf nova oscillations, optical photometry of SS Cyg was obtained with the 2.7-m telescope at McDonald Observatory and the Stiening high-speed photometer on the nights of 1996 October 13, 14, and 15 UT. The Stiening photometer simultaneously measures the flux in four bandpasses similar to the Johnson *UBVR* bandpasses (see Robinson et al. 1995 for the effective wavelengths and widths of the bandpasses). Fluxes were calibrated using the standard star BD+28°4211, and the time standard was UTC as given by a GPS receiver located at the dome of the telescope. The start times of the observations were $\text{JD} - 2450000 = 369.583, 370.644$, and 371.587 ; the run lengths were 3.14, 1.37, and 3.97 hr respectively; and sample intervals were 0.5 s throughout. SS Cyg was observed to fade by ~ 0.25 mag between the first and second nights and by another ~ 0.30 mag between the second and third nights, but the mean flux ratios remained nearly constant from night to night: the F_{ν} flux ratios are $F_U/F_V \approx 1.30$, $F_B/F_V \approx 1.13$, and $F_R/F_V = 0.87$, with $V = 9.04, 9.27$, and 9.56 for October 13, 14, and 15 UT, respectively.

A search was made for optical oscillations by calculating the power spectra of the light curves in the various bandpasses. We found no detectable periodicities in the light curves from the first night with an upper limit on the relative amplitude $\Delta F/F < 3.0 \times 10^{-4}$ for any periodicity between 2.5 s and 10 s. Oscillations were detected on the second and third nights with periods of 6.58 s and 6.94 s, respectively. The mean properties of these oscillations are listed in Table 1. The fluxes in that table should be accurate to a few percent, and the oscillation amplitudes from the third night also should be accurate to a few percent, but on the second night the accuracy of the amplitude measurements are no better than $\sim 20\%$ because the light curves are weak and contaminated by noise so the oscillation amplitudes are poorly determined and biased upwards by noise.

The band fluxes F , oscillation amplitudes ΔF , and relative amplitudes $\Delta F/F$ from the third night are plotted in Figure 3, where it is apparent that the continuum flux of SS Cyg rises monotonically from R through U , while the absolute and hence the relative oscillation amplitudes are smallest in V . As shown by the dotted line, the UBV spectral distribution of the oscillation amplitudes is reasonably consistent with Rayleigh-Jeans, whereas the spectral distribution of the continuum is much flatter: an unweighted fit to the UBV measurements of the oscillation amplitudes and continuum assuming a function of the form $F_\nu \propto \lambda^{-\alpha}$ yields $\alpha = 1.9$ and 0.57 , respectively.

2.3. Optical and EUV

To compare the periods of the oscillations detected in the EUV and optical, we added the points for the optical periods to the lower panel of Figure 1. The period of the oscillation on the second night is about what one would expect from an extrapolation of the *EUVE* data, but, more importantly, the period of the oscillation on the third night is consistent with the value measured contemporaneously by *EUVE*. To investigate this further, we focused the analysis on that (unfortunately short) interval when optical and *EUVE* data were obtained simultaneously: during $JD - 2450000 = 371.6639 - 371.6724$ and $371.7297 - 371.7417$; two stretches of strictly simultaneous observations separated by an *EUVE* orbit. Given the low amplitude of the optical oscillations, we calculated power spectra of the various bands in the encompassing interval $JD - 2450000 = 371.6639 - 371.7417$. For the *EUVE* data, we calculated the power spectra separately for the two intervals. These spectra are plotted in the left panels of Figure 4 (where the EUV power spectrum is the average of the two intervals). In each case (four optical bands, two EUV intervals), the period of the oscillation is found to be 6.94 s (actually, 6.944 ± 0.004 s for the optical channels, 6.94 ± 0.02 s for the EUV channel; the higher accuracy for the optical channels is due to longer data interval). To determine the relative phase of these oscillations, we phase-folded the data assumed a common period of 6.94 s and a common zero point at $JD - 2450000 = 371.7$, midway between the two data intervals. Fitting a sine wave $F + \Delta F \sin 2\pi(\phi - \phi_0)$ to each band separately, we derived the parameters listed in Table 2; the phase-folded light curves and sinusoidal fits are shown in the right panels of Figure 4. The primary result from these efforts is that the relative phase of the oscillation is the same for all the bands. In particular, the phase of the EUV and optical oscillations are the same within the errors: the difference is $\Delta\phi_0 = 0.014 \pm 0.038$. The relative amplitudes derived by these means are higher than derived in the previous section, but it is to be expected that higher amplitudes will be derived over short intervals when the oscillation period is more nearly constant. As before, the oscillation amplitude is highest in U , lowest in V , and comparable at an intermediate value in B and R .

3. Summary and Discussion

We have described EUV and optical photometric observations of SS Cyg obtained during its 1996 October outburst. During the rise to outburst, the period of the EUV oscillation was observed to fall from 7.81 s to 6.59 s over an interval of 4.92 hr, *jump* to 2.91 s, and then fall to 2.85 s over an interval of 4.92 hr. During the decline from outburst, the period of the EUV oscillation was observed to rise from 6.73 s to 8.23 s over an interval of 2.10 days. Optical oscillations were detected on the second and third nights of observations during the decline from outburst with periods of 6.58 s and 6.94 s, respectively. During the times of overlap between the optical and EUV observations on the third night, the oscillations were found to have the same period and phase; they differ only in their amplitudes, which are 34% in the EUV and 0.05%–0.1% in the optical.

The first striking aspect of these observations is the frequency doubling observed on the rise to outburst. SS Cyg appears to have undergone a “phase transition” at a critical period $P_c \lesssim 6.5$ s, when the frequency of its oscillation doubled (Fig. 1) and the “stiffness” of its period-intensity relation ($P \propto I^{-\alpha}$) increased by a factor of ≈ 5 in the exponent (Fig. 2). Optical oscillations were detected on the second and third nights of observations at periods above P_c , but not on the first night when an extrapolation of the trend would predict an oscillation period below P_c . It is interesting to speculate that the optical oscillations of SS Cyg (and possibly other dwarf novae) disappear on the rise to outburst when (if) the source makes the transition to the higher oscillation frequency and “stiffer” period-intensity state, and then reappear on the decline from outburst when the source reverts back to its normal state. Additional simultaneous optical and EUV/soft X-ray observations are required to determine if this is the case. Such observations are also required to determine if this transition takes place at the same period on the rise to and decline from outburst, or whether there is a “hysteresis” in the transition. The observational data are consistent with SS Cyg pulsating at a fundamental period $P \gtrsim 6.5$ s, then switching to a first harmonic and stiffening its period-intensity (by inference period- \dot{M}) relationship so as to avoid oscillating faster than $P_{\min}/2 \approx 2.8$ s. This minimum period $P_{\min} \approx 5.6$ s is consistent with the Keplerian period at the inner edge of the accretion disk if, as seems to be the case observationally, the binary inclination $i \approx 40^\circ$ and the mass of the white dwarf $M_{\text{wd}} \approx 1 M_\odot$. A secure white dwarf mass would confirm this interpretation.

The second striking aspect of these observations is the lack of a phase delay between the EUV and optical oscillations measured simultaneously on the third night (Fig 4). The relative phase delay $\Delta\phi_0 = 0.014 \pm 0.038$ for $P = 6.94$ s, or $\Delta t = 0.10 \pm 0.26$ s. The 3σ upper limit $\Delta t \leq 0.88$ s corresponds to a distance $r = c\Delta t \leq 2.6 \times 10^{10}$ cm. If the EUV oscillation originates near the white dwarf, and the optical oscillation is formed by reprocessing of EUV flux in the surface of the accretion disk, the delays $\Delta t = r(1 - \sin i \cos \varphi)/c$, where the binary inclination $i \approx 40^\circ$ and $0 \leq \varphi \leq \pi$ is the azimuthal angle from the line of sight. Then, the distance to the reprocessing site $r = c\Delta t/(1 - \sin i \cos \varphi) \leq 1.6 \times 10^{10}$ cm. To give a sense of scale, this is about 30 white dwarf radii or one-third the size of the disk. In contrast, eclipse observations of UX UMa (Nather & Robinson 1974; Knigge et al. 1998), Z Cha (Warner & Brickhill 1978), and HT Cas (Patterson

1981) indicate that in these high- \dot{M} cataclysmic variables much or all of the disk contributes to the optical oscillations. The much smaller size of the optical emission region in SS Cyg is derived from an application of echo mapping, made possible for the first time by our strictly simultaneous optical and EUV observations.

The other diagnostic of the optical oscillations is their spectrum, which is nearly Rayleigh-Jeans in UBV (Fig. 3). Given this result, it is interesting to ask if the UBV oscillations of SS Cyg are simply due to the Rayleigh-Jeans tail of the spectrum responsible for the EUV oscillations. Mauche, Raymond, & Mattei (1995) discuss the EUV spectrum of SS Cyg and show that it can be parameterized in the 72–130 Å *EUVE* SW bandpass by a blackbody absorbed by a column density of neutral material. Acceptable fits to the spectrum are possible for a wide range of temperatures kT_{bb} , hydrogen column densities N_{H} , and luminosities L_{bb} , but the tight correlation between these parameters significantly constrains the allowed region of parameter space. From Figures 8–10 of Mauche, Raymond, & Mattei, a reasonable set of acceptable parameters is as listed in the first three columns of Table 3, where we have assumed a source distance $d = 75$ pc and a fiducial SW count rate of 0.5 counts s^{-1} . Scaling to the SW count rate of 0.083 counts s^{-1} observed during the interval of overlap on the third night of observations, the fractional emitting area of these blackbodies $f = L_{\text{bb}}/4\pi R_{\text{wd}}^2 \sigma T_{\text{bb}}^4$ are as listed in the fourth column of Table 3 for an assumed white dwarf radius $R_{\text{wd}} = 5.8 \times 10^8$ cm. With the exception of the coolest model, these fractional emitting areas are smaller than the value $f = H_{\text{bl}}/R_{\text{wd}} \sim 3 \times 10^{-3}$ expected for a boundary layer with a scale height H_{bl} . The B band flux densities M_B of these models are as listed in the fifth column of Table 3, and after multiplying by the EUV oscillation amplitude of 34% they become the oscillation amplitudes ΔM_B listed in the sixth column of Table 3. With an observed oscillation amplitude $\Delta F_B = 4.4 \times 10^{-4}$ Jy (Table 2), the relative model oscillation amplitudes $\Delta M_B/\Delta F_B$ are as listed in the seventh column of Table 3. We conclude that a single source can (within a factor of $\lesssim 3$) produce both the EUV and UBV oscillations of SS Cyg if its boundary layer temperature $kT_{\text{bb}} \lesssim 15$ eV and hence its luminosity $L_{\text{bb}} \gtrsim 1.2 \times 10^{34} (d/75 \text{ pc})^2 \text{ erg s}^{-1}$. Unfortunately, other data cannot confirm or exclude this possibility. First, while blackbody fits to *HEAO 1* LED 1 and *ROSAT* PSPC soft X-ray spectra favor temperatures $kT_{\text{bb}} \approx 20$ –30 eV, they are not *inconsistent* with temperatures as low as $kT_{\text{bb}} \approx 15$ eV (Córdova et al. 1980; Ponman et al. 1995). Second, while the strength of the He II $\lambda 4686$ emission line at the peak of the outburst implies a boundary layer luminosity $L_{\text{bb}} \approx 5 \times 10^{33} (d/75 \text{ pc})^2 \text{ erg s}^{-1}$, hence $kT_{\text{bb}} \approx 20$ eV, the luminosity can be increased to the required value if the fraction of the boundary layer luminosity intercepted by the disk is decreased from $\eta = 10\%$ to $\eta \approx 2\%$; such a model has the added charm of producing the *expected* boundary layer luminosity $L_{\text{bl}} \approx L_{\text{disk}} \approx GM_{\text{wd}}\dot{M}/2R_{\text{wd}} \approx 3 \times 10^{34} (d/75 \text{ pc})^2 \text{ erg s}^{-1}$ (Mauche, Raymond, & Mattei). The recent *Chandra* LETG spectrum of SS Cyg in outburst will better constrain the boundary layer parameters, hence allow us to determine if the boundary layer can produce both the EUV and UBV oscillations.

Either way, we are left to explain the enhancement of the oscillation amplitude in R over that predicted by Rayleigh-Jeans spectrum (Fig. 3). We have no compelling explanation for

this datum, but the echo mapping constraint from above still applies, so the source of the extra oscillation amplitude in R must lie within the inner third of the accretion disk. We note that Steeghs et al. (2001) recently measured the spectrum of the optical oscillations of the dwarf nova V2051 Oph in outburst and found that the oscillation amplitudes of the Balmer and He I emission lines were stronger than the continuum by factors of $\lesssim 5$. Our R bandpass contains the H α emission line, so it is interesting to speculate that the enhanced oscillation amplitude in R might be due to the larger oscillation amplitude of the H α line flux compared to the continuum. Unfortunately, it seems unlikely that the needed factor-of-two enhancement can be produced this way. Also, for this explanation to work, the higher-order Balmer lines must not significantly enhance the oscillation amplitude in B . Fast optical spectroscopy of SS Cyg in outburst is required to determine if this scenario can explain the enhanced oscillation amplitude in R , and, more generally, to determine if our explanation of the origin of the UBV oscillations is correct. Clearly, there is much more observational work to be done.

The *EUVE* observations of SS Cyg could not have been accomplished without the efforts of the members, staff, and director, J. Mattei, of the American Association of Variable Star Observers; *EUVE* Deputy Project Scientist R. Oliverson; *EUVE* Science Planner B. Roberts; the staff of the *EUVE* Science Operations Center at CEA, and the Flight Operations Team at Goddard Space Flight Center. We thank the referee for a number of suggestions which improved the clarity of the manuscript. C. W. M.’s contribution to this work was performed under the auspices of the U.S. Department of Energy by University of California Lawrence Livermore National Laboratory under contract No. W-7405-Eng-48.

REFERENCES

B bowyer, S., et al. 1994, *ApJS*, 93, 569

B bowyer, S., & Malina, R. F. 1991, in *Extreme Ultraviolet Astronomy*, ed. R. F. Malina & S. Bowyer (New York: Pergamon), 397

C órdova, F. A., Chester, T. J., Mason, K. O., Kahn, S. M., & Garmire, G. P. 1984, *ApJ*, 278, 739

C órdova, F. A., Chester, T. J., Tuohy, I. R., & Garmire, G. P. 1980, *ApJ*, 235, 163

F riend, M T., Martin, J. S., Smith, R. C., & Jones, D. H. P. 1990, *MNRAS*, 246, 654

H essman, F. V., Robinson, E. L., Nather, R. E., & Zhang, E.-H. 1984, *ApJ*, 286, 747

H ildebrand, R. H., Spillar, E. J., & Stiening, R. F. 1981, *ApJ*, 243, 223

H orne, K., & Gomer, R. 1980, *ApJ*, 237, 845

J ones, M. H., & Watson, M. G. 1992, *MNRAS*, 257, 633

K nigge, C., Drake, N., Long, K. S., Wade, R. A., Horne, K., & Baptista, R. 1998, *ApJ*, 499, 429

M artínez-Pais, I. G., Giovannelli, F., Rossi, C., & Gaudenzi, S. 1994, *A&A*, 291, 455

M auche, C. W. 1996, *ApJ*, 463, L87

M auche, C. W. 1997, in *Accretion Phenomena and Related Outflows*, ed. D. T. Wickramasinghe, L. Ferrario, & G. V. Bicknell (San Francisco: ASP), 251

M auche, C. W. 1998, in *Wild Stars in the Old West*, ed. S. Howell, E. Kuulkers, C. Woodward (San Francisco: ASP), 113

M auche, C. W., Mattei, J. A., & Bateson, F. M. 2001, in *Evolution of Binary and Multiple Stars*, ed. P. Podsiadlowski, et al. (San Francisco: ASP), 367

M auche, C. W., Raymond, J. C., & Mattei, J. A. 1995, *ApJ*, 446, 842

N other, R. E., & Robinson, E. L. 1974, *ApJ*, 190, 637

N auenberg, M. 1972, *MNRAS*, 254, 493

P atterson, J. 1981, *ApJS*, 45, 517

P atterson, J., Robinson, E. L., & Kiplinger, A. L. 1978, *ApJ*, 226, L137

P onman, T. J., et al. 1995, *MNRAS*, 276, 495

R obinson, E. L., et al. 1995, *ApJ*, 438, 908

Steeghs, D., O'Brien, K., Horne, K., Gomer, R., & Oke, J. B. 2001, *A&A*, 323, 484

van Teeseling, A. 1997, *A&A*, 324, L73

Warner, B. 1995a, *Cataclysmic Variable Stars* (Cambridge: CUP)

Warner, B. 1995b, in *Cape Workshop on Magnetic Cataclysmic Variables*, ed. D. A. H. Buckley & B. Warner (San Francisco: ASP), 343

Warner, B., & Brickhill, A. J. 1978, *MNRAS*, 182, 777

Wheatley, P. J., Mauche, C. W., & Mattei, J. A. 2000, *New Astro. Rev.*, 44, P33

Table 1. Mean Properties of the Optical Oscillations

Date (JD - 2450000)	Period (s)	Band- pass	Flux F (Jy)	Amplitude ΔF (Jy)	Relative Amplitude $\Delta F/F$
370.644–370.701 . . .	6.58	U	0.94	2.6×10^{-4}	2.7×10^{-4}
		B	0.81	1.1×10^{-4}	1.3×10^{-4}
		V	0.72	0.8×10^{-4}	1.1×10^{-4}
		R	0.63	1.0×10^{-4}	1.6×10^{-4}
371.586–371.752 . . .	6.94	U	0.70	3.7×10^{-4}	5.3×10^{-4}
		B	0.62	2.3×10^{-4}	3.7×10^{-4}
		V	0.55	1.6×10^{-4}	2.9×10^{-4}
		R	0.48	1.9×10^{-4}	3.9×10^{-4}

Table 2. Parameters of the Simultaneous EUV and Optical Oscillations

Band-pass	Flux F^a	Amplitude ΔF^a	Relative Amplitude $\Delta F/F$	Phase ϕ_0
EUV	1.30	0.45 ± 0.04	0.34 ± 0.03	0.561 ± 0.014
U	0.71	$(7.7 \pm 0.6) \times 10^{-4}$	$(10.8 \pm 0.9) \times 10^{-4}$	0.577 ± 0.013
B	0.62	$(4.4 \pm 0.4) \times 10^{-4}$	$(7.1 \pm 0.6) \times 10^{-4}$	0.578 ± 0.014
V	0.56	$(2.8 \pm 0.4) \times 10^{-4}$	$(5.0 \pm 0.7) \times 10^{-4}$	0.575 ± 0.022
R	0.48	$(3.4 \pm 0.4) \times 10^{-4}$	$(7.1 \pm 0.9) \times 10^{-4}$	0.567 ± 0.019

^aUnits: DS counts s^{-1} for the EUV band, Jy for the optical bands

Table 3. Blackbody Model Parameters

kT (eV)	N_{H} (cm $^{-2}$)	L_{bb} (erg s $^{-1}$)	f	Flux M_B (Jy)	Amplitude ΔM_B (Jy)	Relative Amplitude $\Delta M_B/\Delta F_B$
15....	9.5×10^{19}	1.2×10^{34}	9.3×10^{-3}	4.3×10^{-4}	1.5×10^{-4}	3.3×10^{-1}
20....	7.0×10^{19}	2.2×10^{33}	5.2×10^{-4}	3.3×10^{-5}	1.1×10^{-5}	2.5×10^{-2}
25....	5.4×10^{19}	8.5×10^{32}	8.3×10^{-5}	6.6×10^{-6}	2.2×10^{-6}	5.1×10^{-3}
30....	4.4×10^{19}	4.7×10^{32}	2.2×10^{-5}	2.1×10^{-6}	7.2×10^{-7}	1.6×10^{-3}
35....	3.7×10^{19}	4.0×10^{32}	1.0×10^{-5}	1.2×10^{-6}	3.9×10^{-7}	8.9×10^{-4}

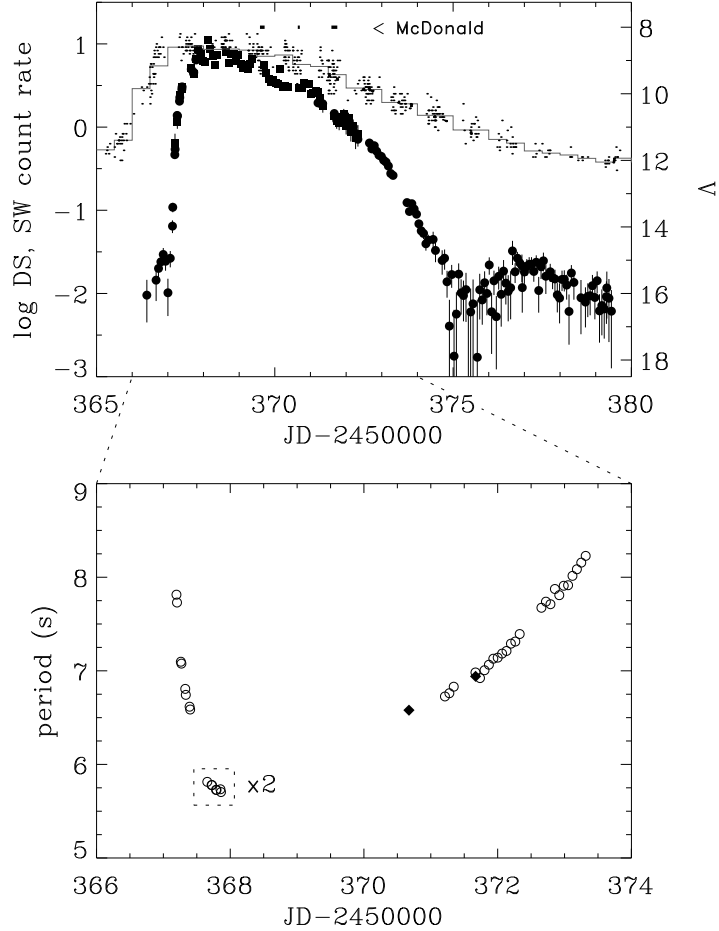


Fig. 1.— *Upper panel:* *EUVE* and AAVSO optical light curves of the 1996 October outburst of SS Cyg. DS and SW measurements are shown respectively by the filled circles and squares with error bars; individual AAVSO measurements are shown by the small dots; 0.5 day mean optical light curve is shown by the histogram. Intervals of observations at McDonald Observatory are indicated by the thick bars. *Lower panel:* Oscillation period versus time. *EUVE* DS and McDonald Observatory optical measurements are shown by the open circles and filled diamonds, respectively. Points enclosed by the dotted box are plotted at twice the observed periods.

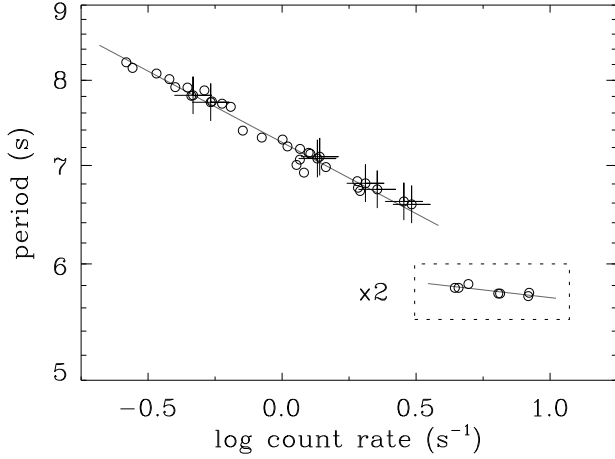


Fig. 2.— Period of the EUV oscillation as a function of DS count rate. Points on the rising branch of the outburst are distinguished with crosses. Grey lines are the unweighted fits to the data: $P = 7.26 I^{-0.097}$ s and $P = 2.99 I^{-0.021}$ s. Points enclosed by the dotted box are plotted at twice the observed periods.

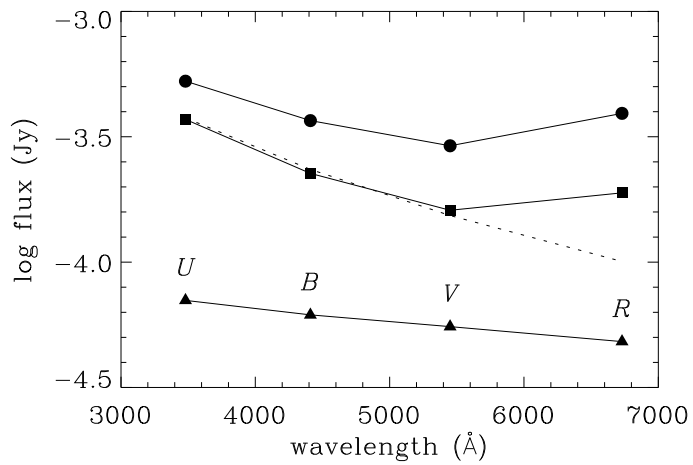


Fig. 3.— Optical flux ($F/10^4$, filled triangles), oscillation amplitude (ΔF , filled squares), and relative oscillation amplitude ($\Delta F/F$, filled circles) for 1996 October 15 UT. Dotted line is a Rayleigh-Jeans spectrum normalized to the UBV fluxes of the oscillation amplitude.

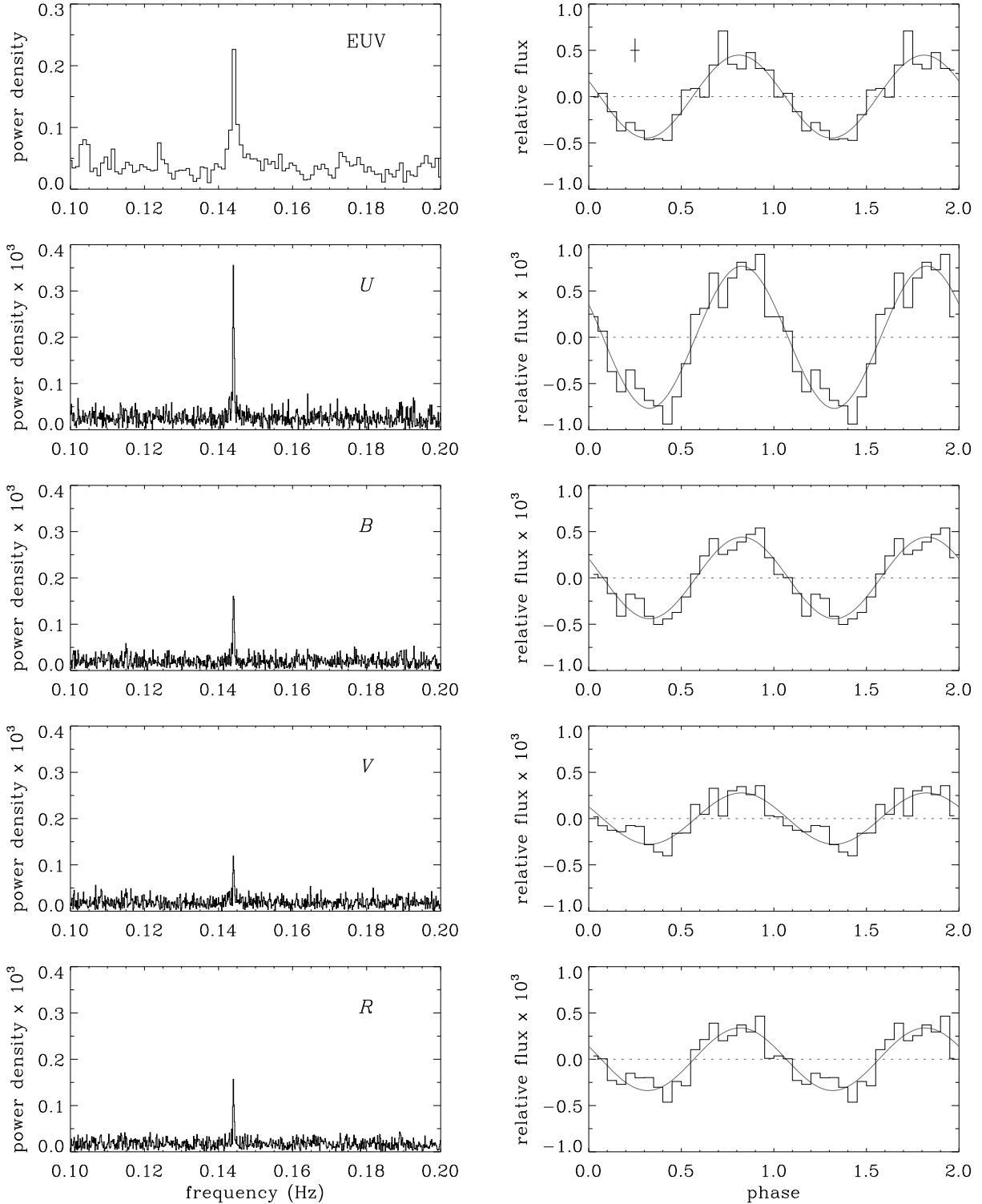


Fig. 4.— Power density (*left panels*) and phase-folded light curves (*right panels*) of SS Cyg in the EUV and optical U , B , V , and R for the intervals of overlap on 1996 October 15 UT. Typical error bar for the EUV light curve is shown by the cross, and the sinusoidal fits are the grey curves.